Journal of Thermal Analysis and Calorimetry, Vol. 89 (2007) 2, 465–473

EXPLORING THE PHYSICAL, CHEMICAL AND THERMAL CHARACTERISTICS OF A NEW POTENTIALLY INSENSITIVE HIGH EXPLOSIVE RX-55-AE-5

R. K. Weese, A. K. Burnham[*]*, Heidi C. Turner and T. D. Tran*

Energetic Materials Center, Chemistry and Materials Science Directorate, Lawrence Livermore National Laboratory
P. O. Box 808, L-282, California, 94551, USA

Current work at Lawrence Livermore National Laboratory (LLNL) includes both understanding properties of old explosives and measuring properties of new ones. The necessity to know and understand the properties of energetic materials is driven by the need to improve performance and enhance stability to various stimuli, such as thermal, friction and impact insult.

This paper will concentrate on the physical properties of RX-55-AE-5, which is formulated from heterocyclic explosive, 2,6-diamino-3,5-dinitropyrazine-1-oxide, LLM-105, and 2.5% Viton A. Differential scanning calorimetry (DSC) was used to measure a specific heat capacity, C_p, of ≈0.950 J g^{-1} °C^{-1}, and a thermal conductivity, κ, of ≈0.475 W m^{-1} °C^{-1}. The LLNL kinetics modeling code Kinetics05 and the Advanced Kinetics and Technology Solutions (AKTS) code thermokinetics were both used to calculate Arrhenius kinetics for decomposition of LLM-105. Both obtained an activation energy barrier E≈180 kJ mol^{-1} for mass loss in an open pan. Thermal mechanical analysis, TMA, was used to measure the coefficient of thermal expansion (*CTE*). The *CTE* for this formulation was calculated to be ≈61 μm m^{-1} °C^{-1}. Impact, spark, friction are also reported.

Keywords: *coefficient of thermal expansion, energetic materials, insensitive explosives, specific heat capacity, thermal conductivity, thermal decomposition kinetics*

Introduction

There is a continuing interest in developing explosives with increased performance and safety features [1]. Such development requires extensive characterization of both the explosive molecule itself but also the many possible formulations that enable it to be processed effectively and safely. One of the materials being investigated at the Energetic Materials Center of LLNL is 2,6-diamino-3,5-dinitropyrazine-1-oxide (LLM-105), which is a promising pathway to create potentially less sensitive explosive formulations without undue sacrifice of performance [2, 3].

LLM-105 has a higher energy density than 1,3,5-triamino-2,4,6-trinitrobenzene (TATB). LLM-105 has a density of 1.913 g cm^{-3}, a Dh_{50} of 90–150 cm, and is insensitive to both spark and friction. It has an onset temperature for decomposition of 348°C at a linear heating rate of 10°C min^{-1} as measured by Differential Scanning Calorimetry (DSC). It is generally insoluble in common organic solvents. TATB is well noted for its *CTE* property, ratchet growth [4]; its thermal stability (m.p. >370°C), its low insensitivity to external stimuli, such as drop hammer (which is often referred to as impact), spark, and friction; and its very low solubility in a wide array of solvents.

A new LLM-105 formulation, RX-55-AE-5, has been prepared and subjected to physical characterization tests. RX-55-AE-5 is formulated from 97.5% LLM-105 and 2.5% Viton A. Properties of RX-55-AE-5, LLM-105, and TATB are summarized in Table 1. In this work, we measure and report the thermal expansion coefficient, thermal decomposition kinetics, and sensitivity to spark,

Table 1 Properties of RX-55-AE-5 and other materials for comparison [2–4]

Property	RX-55-AE-5	LLM-105	TATB
Molecular mass/g mol^{-1}	–	216.04	258.2
Color	yellow	yellow	yellow
Crystal structure	–	monoclinic	triclinic
Density/g cm^{-3}	–	1.91	1.94

* Author for correspondence: burnham1@llnl.gov

1388–6150/$20.00

Akadémiai Kiadó, Budapest, Hungary
Springer, Dordrecht, The Netherlands

Table 2 Formulations for RX-55-AE-5, PBX 9502 and LX-17

Material/%	RX-55-AE-5	PBX 9502	LX-17
LLM-105	97.5	–	–
TATB	–	95.0	92.5
Kel-F 800	–	5.0	7.5
Viton A	2.5	–	–

friction, and impact for the RX-55-AE-5 formulation of LLM-105. We compare our results for RX-55-AE-5 to PBX 9502, LX-17 and TATB [4]. PBX 9502 is formulated from 95% TATB and 5% Kel-F 800, and LX-17 is formulated from 92.5% TATB and 7.5% Kel-F 800. Formulations using LLM-105 and TATB are listed in Table 2.

Experimental

Materials

We used RX-55-AE-5, a material synthesized by Phil Pagoria. The designation RX-55-AE-5 refers to a research explosive synthesized and processed at LLNL. This material has not been analyzed for trace quantities of impurities, etc. To our knowledge there is no uniform specification for how to prepare LLM-105 and TATB-based materials. For samples like those prepared here in this work, we used UCRL-ID-119665 [5] as a guide for our sample preparation. It is clear that expansion can be affected by micro-structural properties such as the size of the crystallites, porosity, polymer molecular mass distribution, density, and material purity. Properties such as these are important and affect mechanical properties and should be considered in measuring *CTE* [6]. Three sample pellet sizes were prepared. Sample pellets were pressed uniaxially at 105°C in a conventional compaction die without mold release, using two pressing cycles of 5 min at 200 MPa for the two larger pellets and one cycle for the smallest pellet. The smallest pellet was approximately 20 mg and was used for specific heat capacity measurements. The medium pellet was approximately 0.36 g and was used for coefficient of thermal expansion measurements. The largest pellet was approximately 0.70 g and was used to make thermal diffusivity measurements. Sample densities ranged from 1.74 to ~1.82 g cm^{-3} (91.0 to 95.2% theoretical maximum density (TMD)) [7]. Sample masses and densities are summarized in Table 3.

Apparent specific heat capacity

We measured the apparent specific heat capacity, C_p, using modulated differential scanning calorimetry (MDSC) [8–10]. MDSC measures the difference in the heat flow between a sample and an inert reference measured as a function of time and temperature. MDSC analyses of RX-55-AE-5 were carried out using a TA Instruments Model 2920. A linear heating rate of 3°C per minute was used for all C_p measurements.

Thermal mechanical analysis

We measured the coefficient of thermal expansion, *CTE*, of RX-55-AE-5 using a TA Instruments Model 2940 TMA that was controlled by a TA 500 Thermal Analyzer equipped with a TMA Mechanical Cooling Accessory [11, 12]. A quartz micro-expansion probe sat on top of all samples with a force of 0.01 Newtons (N). The change in the length of the sample as it was heated or cooled was measured by a linear transformer that converted the vertical distance of the quartz motion probe and was recorded by the TA Instrument software. Ultra high purity nitrogen carrier gas was used at a constant flow rate of 100 cm^3 min^{-1}. Samples were heated at a linear heating rate of 3°C min^{-1}.

Temperature, force, probe and cell constant calibrations were carried out as prescribed [12], using NIST standards of indium, lead, tin and zinc metals along with aluminum standard reference material. *CTE* measurements using a NIST certified aluminum standard had less than ±2% drift associated over the temperature range of –20 to 100°C.

Thermal diffusivity measurements

Thermal diffusivity measurements were made using a Netzsch Model LFA 457 laser flash diffusivity apparatus. The apparatus in this work was equipped with a moderate temperature, water-cooled furnace

Table 3 RX-55-AE-5 averaged sample mass, volume, density and dimensions

Sample used for	Length/cm	Diameter/cm	Mass/g	Volume/cm^3	Density/g cm^{-3}
C_p	0.035	0.6330	0.020	0.011	~1.82
CTE	0.642	0.0633	0.356	0.205	1.74
λ	0.307	0.6365	0.699	0.391	1.79

where C_p indicates specific heat capacity, J g^{-1} °C^{-1}, *CTE* indicates coefficient of thermal expansion, μm m^{-1} °C^{-1}, and λ indicates thermal diffusivity, mm^2 s^{-1}

capable of operation from –100 to 600°C. The sample chamber is isolated from the heating element by a protective tube allowing samples to be tested under vacuum or in oxidizing, reducing or inert atmosphere. A single graphite-coating layer was applied to the pellet material. The sample holder can be briefly described as silicone-carbide 12.7 mm centering cone. An applied voltage of approximately 2018 V was used with the beam filter set at 25%. Figure 1 shows voltage *vs.* energy per unit squared supplied courtesy of Netzsch Instruments Company, Germany. All samples were analyzed in a helium atmosphere that purged the system at a constant flow rate of approximately 50 mL min^{-1}. The approximate 0.7 g pressed samples used for thermal diffusivity measurements (Table 2). A thermal diffusivity model described by Netzsch as Cowan plus correction was used to calculate the observed thermal diffusivity and to account for heat lost.

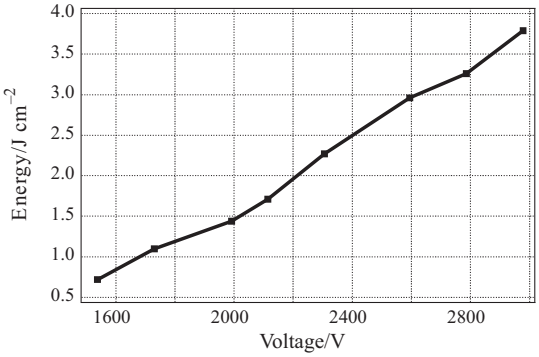

Fig. 1 Bolometer data supplied by Netzsch Instrument Company

Small-scale safety tests

The frictional sensitivity [13] of RX-55-AE-5 was evaluated using a B.A.M. high friction sensitivity tester. The tester employs a fixed porcelain pin and a movable porcelain plate that executes a reciprocating motion. Mass affixed to a torsion arm allows for a variation in applied force between 0.5 and 36.0 kg, and our tests used a contact area of 0.031 cm^2. The relative measure of the frictional sensitivity of a material is based upon the largest pin-load at which less than two ignitions (events) occur in ten trials. No reaction is called a 'no-go', while an observed reaction is called a 'go'.

The sensitivity of RX-55-AE-5 toward electrostatic discharge [14] was measured on a modified Electrical Instrument Services Electrostatic Discharge (ESD) Tester. Samples were loaded into Teflon washers and covered with a 1 mm thick Mylar tape. The density of this packed material was 1.4 cm^3 g^{-1}. The ESD threshold is defined as the highest energy setting at which a reaction occurs for a 1 in 10 series of attempts. Tests were run on powder and pellets at 68°F and a relative humidity of 56%.

An Explosives Research Laboratory Type 12-Drop Weight apparatus [5], more commonly called a 'Drop-Hammer Machine' was used to determine the impact sensitivity relative to the primary calibration materials PETN, RDX, and Comp B-3 at 68°F and 56% relative humidity. The apparatus was equipped with a Type 12A tool and a 2.5 kg mass. The 35±2 mg powder sample was impacted on a Carborundum 'fine' (120 grit) flint paper. A 'go' was defined as a microphone response of 1.3 V or more as measured by a model 415B Digital Peakmeter. A sample population of 15 was used. The mean height for 'go' events, called the '50% Impact Height' or Dh_{50}, was determined using the Bruceton up-down method.

Kinetics

Differential scanning calorimeter, DSC, analyses of RX-55-AE-5 was carried out using a TA Instruments Model 2920. TA Instruments pinhole hermetic aluminum pans were used. The pinhole hermetic pan is a pan that utilizes a small laser perforation in the lid to insure that the pinhole size is uniform and allows the generated gases to escape slowly during decomposition. Samples sizes were limited to <0.5 mg to prevent over-pressure problems. Linear heating rates of approximately 0.1, 0.35 and 1.0°C min^{-1} and a purge gas flow of 50 cm^3 min^{-1} of ultra high purity nitrogen were used for decomposition kinetics.

Mass loss measurements were carried out using a TA Instruments Simultaneous Differential Thermogravimetric Analyzer (SDT), model 2960, manufactured by TA Instruments. TA Instruments open aluminum pans were used. Samples sizes ranged from 0.4 to 0.5 mg. Linear heating rates of approximately 0.1, 0.35 and 1.0°C min^{-1}. Ultra high purity nitrogen gas at a flow rate of 100 cm^3 min^{-1} was used for all SDT analyses. The SDT instrument is capable of performing both thermogravimetric analysis (TG) and differential thermal analysis (DTA) at the same time.

Data were analyzed using the LLNL Kinetics05 program and the AKTS Thermokinetics program.

Results and discussion

Physical properties

Heat capacity values, C_p, measured by MDSC were 0.950, 0.931, 1.098, 1.125 and 0.991 J g^{-1} $°C^{-1}$ for RX-55-AE-5, LLM-105, PBX 9502 LX-17 and TATB, respectively. The thermal diffusivity of

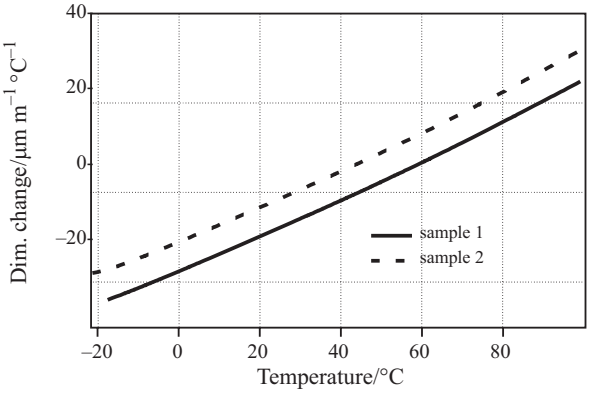

Fig. 2 RX-55-AE-5 dimensional change *vs.* temperature

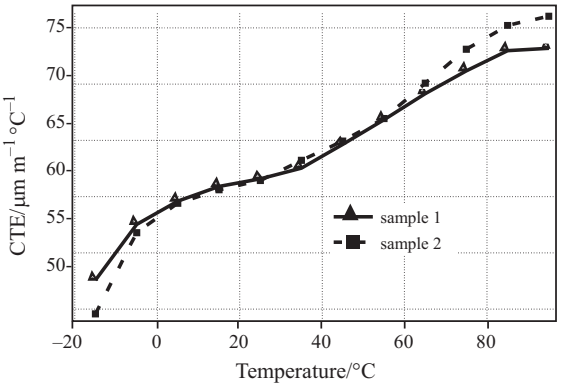

Fig. 3 CTE *vs.* temperature for RX-55-AE-5 over the temperature range of –20 to 100°C

Table 4 RX-55-AE-5 *CTE* values, μm m^{-1} °C^{-1}

Sample	–20°C to 0°C	0°C to 20°C	20°C to 40°C	40°C to 60°C	60°C to 80°C	80°C to 100°C
1	55	60	62	66	70	73
2	56	60	62	66	72	76

RX-55-AE-5 was measured to be 0.264 mm^2 s^{-1} at 20°C. This is the first thermal diffusivity measurement for RX-55-AE-5 to our knowledge.

Figure 2 shows two independent TMA analyses over the temperature range of –20 to 100°C. The two slopes are indistinguishable from one another, so the dimensional change of the two samples is reproducible. *CTE* values were calculated using

$$CTE = \frac{\mathrm{d}L}{\mathrm{d}T^{*}L_{\mathrm{o}}} \tag{1}$$

where dL is the change in length (μm), is the change in temperature (°C), and L_o is the initial sample length (meters). Results are plotted in Fig. 3, and average values are listed in Table 4 for six specific temperature intervals.

Safety properties

Small scale testing (SST) of energetic materials and other compounds is done to determine sensitivity to various stimuli, including friction, impact and static spark [5, 13, 14]. These tests establish parameters for the safety in handling and carrying out experiments that will describe the behavior of materials that are commonly stored for long periods of time. In the friction sensitivity test, RX-55-AE-5 was observed to have 1/10 'goes' at 36.0 kg at 22°C and a relative humidity of 64%. RX-55-AE-5 was compared to an RDX calibration sample, which was also found to have 1 event in 10 trials at 12.4 kg. This material is not considered to be friction sensitive. In the spark sensitivity test, no reactions were observed (0/10) at 10 kV (1 J). This material is not spark sensitive under these specific conditions. In the impact sensitivity test, the Dh_{50} for RX-55-AE-5 was 170±1.0 cm. For comparison, the Dh_{50} of PETN, RDX, and Comp B-3 were measured at 15.5, 34.5 and 41.4 cm, respectively.

Kinetics

For the decomposition kinetics, the conventional starting equation gives the rate of reaction in terms of a rate constant times a function of the extent of reaction:

$$\frac{\mathrm{d}\alpha}{\mathrm{d}t} = k(T)f(\alpha) \tag{2}$$

where $f(\alpha)$ describes the conversion dependence of the rate, and the temperature dependence of k is typically described by an Arrhenius law (k= $A\exp(-E/RT)$), where A is a frequency factor, E is an activation energy, and R is the gas constant.

The simplest methods of kinetic analysis used in Kinetics05 is Kissinger's method [15], in which the shift of temperature of maximum reaction rate (T_{max}) with heating rate (β) is given by

$$\ln(\beta/T_{\max}^{2}) = -E/RT_{\max} + \ln(AR/E) \tag{3}$$

Friedman's isoconversional method [16] involves an Arrhenius analysis at constant levels of conversion, and we determined the apparent first-order frequency factor and activation energy at 1% intervals using both LLNL and AKTS kinetics analysis programs.

Model fitting used the extended Prout–Tompkins model [17],

$$f(\alpha) = (1 - q(1 - \alpha))^m(1 - \alpha)^n \qquad (4)$$

where α is the fraction reacted, n is the reaction order, m is a nucleation-growth parameter, and q is an initiation parameter set equal to 0.99. When m is zero, this model reduces to an n^{th}-order reaction.

For the SDT data, we considered only mass loss for kinetic analysis. Instability of the DTA baseline meant that results were inconclusive as to whether the mass loss corresponds to an endothermic or exothermic process, or some combination thereof, but since the mass loss is complete prior to exothermic reaction in the DSC, we presume it is primarily sublimation. Kissinger's method yielded A=2.19·10^{13} s^{-1} and E=173.5 kJ mol^{-1}, with a standard error of 8.7 kJ mol^{-1} on the activation energy. The Friedman parameters are shown in Fig. 4 and are approximately equal to the Kissinger value.

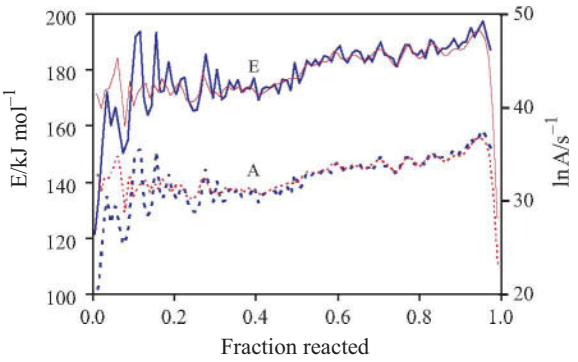

Fig. 4 Conversion dependence of A and E determined by Friedman's method. The bold lines used LLNL Kinetics05 and the thin lines used AKTS Thermokinetics

For the model fitting approach, the shape of the reaction profile – the sharp decline past the maximum reaction rate and the direct approach to baseline – suggests an n^{th}-order reaction with n<1. Simultaneously fitting the three cumulative reaction profiles to such a model gave reaction parameters of A=6.20·10^{13} s^{-1}, E=172.9 kJ mol^{-1}, and n=0.65. A comparison of the measured fractions reacted with those calculated from both the isoconversional and n^{th}-order fits is shown in Fig. 5. The reaction profile is not an ideal n^{th}-order reaction, so the n^{th}-order fit shows significant deviation.

A better fit can be obtained to the latter stages of reaction by fitting the reaction rates instead of the cumulative reacted, but the fit to the early portion of the reaction is worse. Consequently, m was also optimized *vs.* reaction rates, and the results are shown in Fig. 6. The measured and calculated fraction reacted curves are essentially super-imposable.

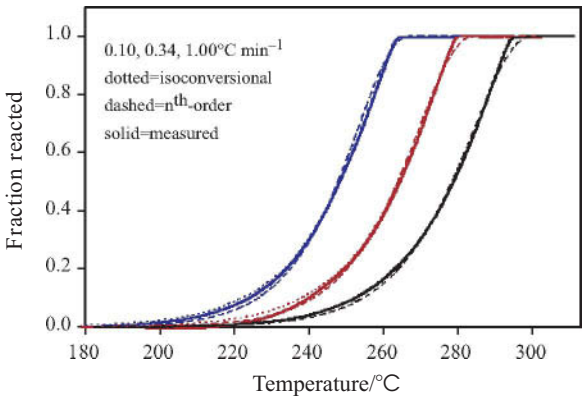

Fig. 5 Comparison of integrated experimental data with that calculated from the isoconversional and n^{th}-order fits

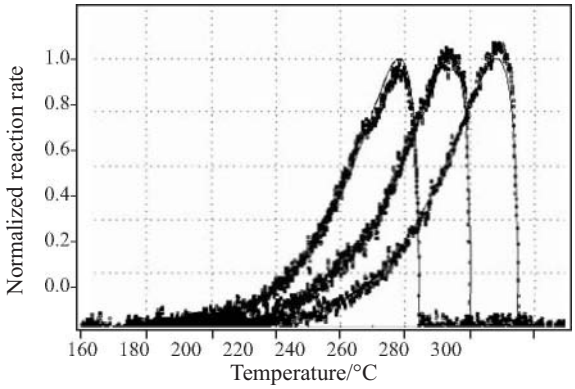

Fig. 6 Comparison of measured reaction rates with those calculated from a fit to an extended Prout–Tompkins model, with A=9.06·10^{13} s^{-1}, E=182.8 kJ mol^{-1}, n=0.315, and m= –0.32

The negative nucleation-growth parameter has no physical meaning; it merely serves as a method of fitting the profile shape and width simultaneously.

The DSC experiments varied in peak shape, possibly due to confinement conditions of the sample. DSC analyses were carried out at linear heating rates of 0.1, 0.35 and 1.0°C min^{-1}. Replicated runs at each temperature were evaluated. The most run deemed most representative of pinhole hermetic pan conditions was analyzed using the Kissinger and Friedman methods. Kissinger's method gave A=7.79·10^{19} s^{-1} and E=263.2 kJ mol^{-1}, with a standard error of 7.7 kJ mol^{-1} on the activation energy. The Friedman parameters are shown in Fig. 7 and a comparison of measured and calculated reaction rates is given in Fig. 8. The activation energy varies generally between 250 and 350 kJ mol^{-1}, and values in the early-mid conversion range agree with Kissinger's method.

Our *CTE* determinations of RX-55-AE-5 as a function of temperature agree well with each other. There are no published data on this new formulation, so we cannot compare to literature results. We can compare our RX-55-AE-5 results to those for LX-17 and PBX 9502 formulations for which our new

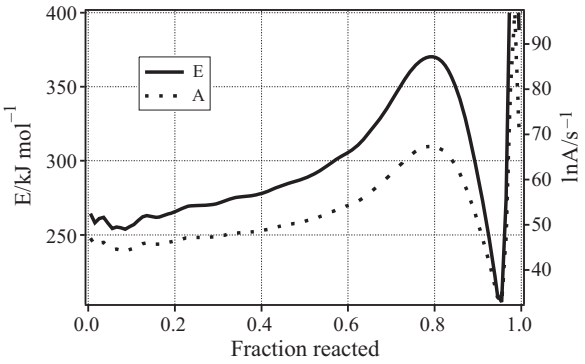

Fig. 7 Friedman isoconversional kinetic parameters for DSC heat release from RX-55-AE-5 heated at 0.1, 0.35 and 1.0°C min^{-1} in a pinhole hermetic pan

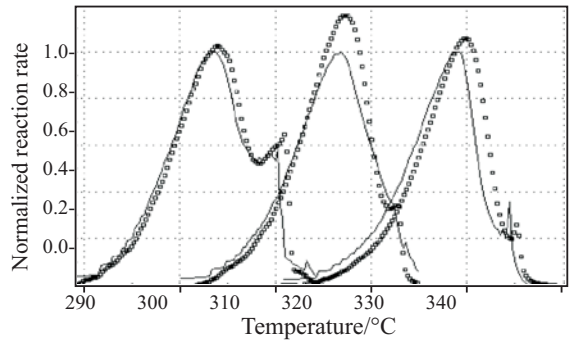

Fig. 8 Comparison of measured and calculated reaction rates of RX-55-AE-5 using Friedman's method at linear heating rates of 0.1, 0.35 and 1.0°C min^{-1}

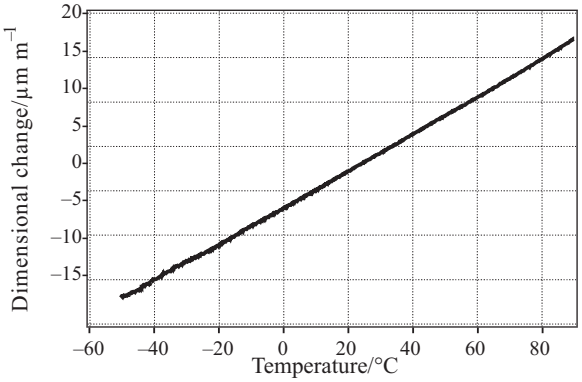

Fig. 9 RX-55-AE-5 dimensional change as a function of temperature

material is intended to replace. Figure 9 shows the observed dimensional changes *vs.* temperature for RX-55-AE-5, and Fig. 10 compares those results to values for TATB, LX-17 and PBX 9502.

Figure 11 shows averaged *CTE* data for RX-55-AE-5, LX-17 and PBX 9502 over the temperature range of –25 to 75°C. Other parameters, such as particle size, wet aminated or dry aminated, should be considered, but they were not varied in the present work. Previous works by Maienschein and

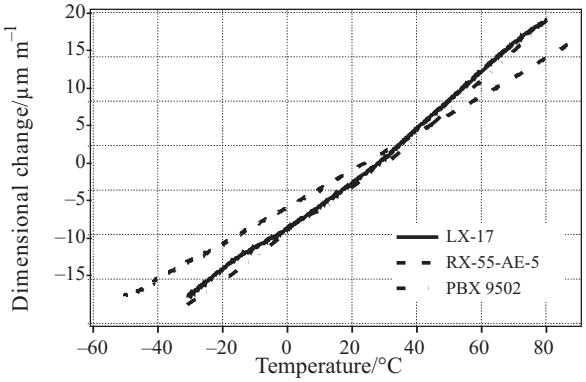

Fig. 10 Overlay of dimensional change for RX-55-AE-5, LX-17 and PBX 9502

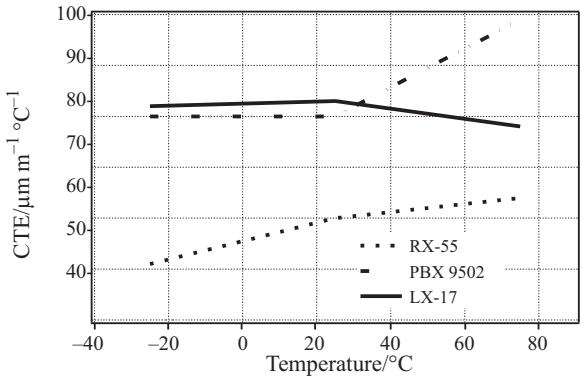

Fig. 11 *CTE* plotted values for RX-55-AE-5, LX-17 and PBX 9502

Garcia [18] show that variations in *CTE* values can result from factors such as pressing at elevated temperature *vs.* room temperature. Apparent residual strain is incorporated into the sample from the sample pressing process and is released during heating. Irreversible ratchet growth was observed in LX-17 when thermally cycled and continued to expand when held between 250–285°C for 4–5 h.

Variation in the *CTE* values for PBX 9502 was not the focus of this work; rather it was how the *CTE* values for RX-55-AE-5 compare to LX-17 and PBX 9502, IHE materials. The comparison of RX-55-AE-5, LX-17 and PBX 9502 in Table 5 shows that RX-55-AE-5's *CTE* values change the least over the temperature range of –25 to 75°C. Figure 11 makes this comparison graphically. PBX 9502 and LX-17 have similar slopes at lower temperatures. The *CTE* of RX-55-AE-5 is between the two TATB

Table 5 Averaged CTE values (μm m^{-1} °C^{-1}) for RX-55-AE-5, LX-17 and PBX 9502

Temp./°C	RX-55-AE-5	LX-17	PBX 9502
–25	50	82	80
25	60	83	80
75	64	78	99

formulations at –25°C, its weaker temperature dependence makes its *CTE* substantially smaller than either LX-17 or PBX 9502 at 75°C. It should be mentioned that certain characteristics of *CTE* slopes for compounds such as these are reduced when only three points are plotted. Curves that include many more points will often reveal transitions such as T_g.

Table 6 compares the Small Scale Safety Test (SST) values for RX-55-AE-5, TATB, LX-17 and PBX 9502 that were determined in this work. Thermal decomposition is used to determine the thermal stability of a material with respect to temperature. TATB compounds are well known for their stability towards heat and are known to decompose at temperatures that range from approximately 370 to 385°C when heated at rates of 3 to 10°C min^{-1}. Figures 12 and 13 compare DSC thermal decomposition scans of RX-55-AE-5 with those of TATB, LX-17 and PBX 9502 for thermal stability comparison. RX-55-AE-5 has a much broader decomposition peak than the TATB compounds. It is not understood why the decomposition peak is so broad and appears to have at least two peaks present.

Chemical Reactivity Test, CRT, is a test used at LLNL to quantify gas generation at 80, 100 and 120°C, depending on the material(s). Although not presented in this work, initial CRT testing shows that RX-55-AE-5 is comparable to LX-17 and PBX 9502.

Table 6 summarizes the sensitivity to friction (B.A.M.) tests for RX-55-AE-5, LLM-105, TATB, LX-17 and PBX 9502. RX-55-AE-5 showed no sensitivity to friction by the method we used in this experiment [13]. The ESD threshold of 1.0 J of energy applied to or RX-55-AE-5 and the other comparison materials showed no reaction to electrical stimuli under the conditions used.

Dh_{50} for RX-55-AE-5 was slightly higher than the pure LLM-105 material and slightly lower than that of TATB, LX-17 and PBX 9502. Drop hammer testing of RX-55-AE-5 has been carried out at other laboratories. Pantex, Amarillo, Texas, reports a Dh_{50} of 147 cm. Indian Head, Maryland, reports a Dh_{50}

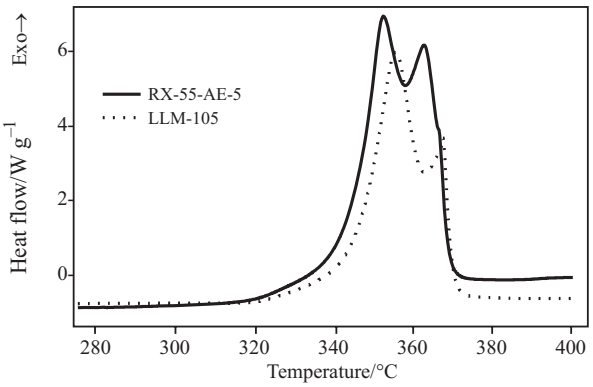

Fig. 12 Overlay of DSC decomposition scans of RX-55-AE-5 and LLM-105 at a linear heating rate of 10°C min^{-1}

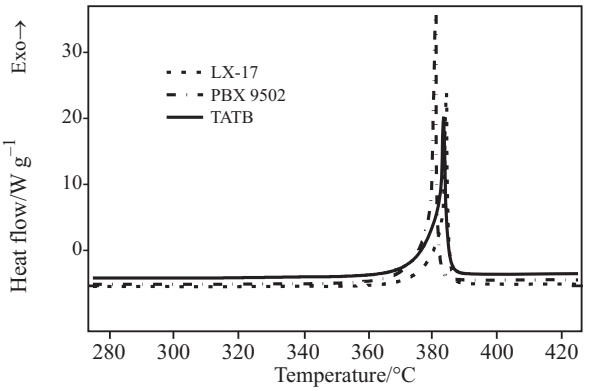

Fig. 13 Overlay of DSC decomposition scans of TATB, LX-17 and PBX 9502 at a linear heating rate of 10°C min^{-1}

Table 6 Summary of test results

Test	RX-55-AE-5	LLM 105	PBX 9502	LX-17	TATB
DSC (onset of exotherm/°C)	352/363	356/367	381	384	384
Friction (no. of goes) at 36 kg	0/10	0/10	0/10	0/10	0/10
ESD treshold (1.0 J)	0/10	0/10	0/10	0/10	0/10
Dh_{50}/cm	170	158	>177	>177	>177
E/kJ mol^{-1}[(2)]	263	250	201	184	193
C_p/J g^{-1} °C^{-1}	0.950	0.931	1.098	1.125	0.991
λ/mm^2 s^{-1} at 26.85°C	0.270	[(1)]	0.404	0.410	0.405
κ/W m^{-1} °C^{-1} 2 26.85°C	0.475	[(1)]	0.789	0.747	0.777
CTE/μm m^{-1} °C^{-1} at 21°C	61	[(1)]	90	80	85

[(1)]Unable to press pellets from powder and perform physical measurement on material, [(2)]Kinetics05 used to calculate results using the isoconversional method for DSC linear heating rates

range of 90–165 cm, while LLNL reports Dh_{50} range of 90–170 cm.

Comparison of the reaction rates in Figs 6 and 8 indicated that the heat release in a sealed pinhole hermetic pan occurs at ~45°C higher than mass loss in open pans, suggesting that sublimation reactions are reduced and decomposition reactions are enhanced. This is also reflected in a ~90 kJ mol^{-1} increase in the activation energy deduced from a comparison of Figs 4 and 7.

The decomposition temperatures for RX-55-AE-5, LX-17 and PBX 9502 reported in Table 6 indicate that the thermal stability of RX-55-AE-5's first decomposition peak T_{max} is approximately 30 to 32°C less than the TATB compounds T_{max}. Figure 12 compares the decomposition temperatures of RX-55-AE-5 and LLM-105. Figure 13 compares TATB, LX-17 and PBX 9502 decomposition temperatures. TATB, LX-17 and PBX 9502 are almost indistinguishable from one another with PBX 9502 being slightly less than TATB or LX-17. RX-55-AE-5 and LLM-105 decomposition peak shapes are indistinguishable from one another. Their shapes are similar in so much as they both show two decomposition peaks. Figure 12 shows that first and second decomposition peaks of LLM-105 are slightly higher (4°C) than the RX-55-AE-5. The two peaks observed in the decomposition of RX-55-AE-5 and LLM-105 are somewhat suspect at this time. There has not been a set of tests defined to determine the impurity content for these research compounds, RX-55-AE-5 and LLM-105. Impurities from synthesis, processing, etc. could be present and therefore affect decomposition temperatures and peak shapes. The decomposition peak of the RX-55-AE-5 is broad, ~50°C. This broad temperature range over which the RX-55-AE-5 and LLM-105 decompose is not typical of TATB type materials (~20°C) compared here in this work. Although not shown in this work, it should be noted that the compound 2,2-bis[(nitroxy)methyl]-1,3-propanediol dinitrate, commonly referred to as PETN, has a base width for its decomposition peak comparable to that of RX-55-AE-5.

Kinetics05 modeling program was used to calculate decomposition kinetics for this set of insensitive high explosives, IHE's. The LLM-105 energy of activation barrier was observed to be approximately 13 kJ mol^{-1} lower than the RX-55-AE-5 that contains approximately 2.5% Viton A as a binder. Other works by Gupa and associates [19] have shown that binder concentrations can lower the activation barrier. Calculated energy of activation barrier for TATB was observed to be approximately 193 kJ mol^{-1} while LX-17 was

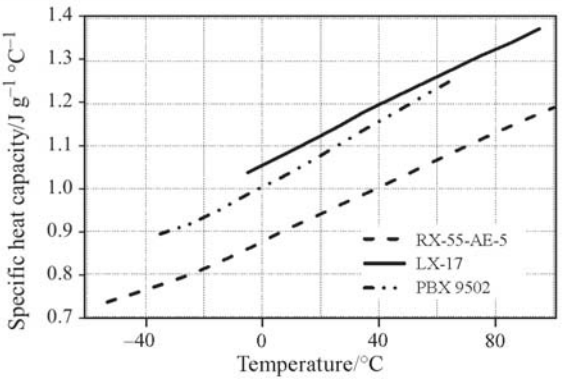

Fig. 14 Heat capacity of RX-55-AE-5, PBX 9502 and LX-17 *vs.* temperature

184 kJ mol^{-1} and PBX 9502 is reported with the highest energy of activation barrier of 201 kJ mol^{-1}. Since LX-17 is 92.5% TATB and 2.5% Kel-F 800 and PBX 9502 is 95% TATB and 5% Kel-F 800, the values reported in Table 6 prove that these values are probably indistinguishable from one another.

The heat capacity of RX-55-AE-5, LX-17 and PBX 9502 is shown in Fig. 14. The heat capacity of RX-55-AE-5 is less than LX-17 and PBX 9502. Heat capacity for LX-17 is slightly higher than PBX 9502.

The results listed in Table 7 show that C_p, κ and *CTE* values for TATB compounds are slightly higher than for RX-55-AE-5. RX-55-AE-5 compares well to LX-17 and PBX 9502.

Acknowledgements

We would like to thank Dr. Craig Tarver and Dr. Phil Pagoria for their technical discussions, help and support on this project. This work performed under the auspices of the U.S. Department of Energy by the University of California, Lawrence Livermore National Laboratory, under Contract number W-7405-Eng-48.

References

1 J. S. Lee and K. S. Jaw, J. Therm. Anal. Cal., 85 (2006) 463.
2 C. M. Tarver, P. A. Urtiew and T. D. Tran, J. Energ. Mater., 23 (2005) 183.
3 P. F. Pagoria, G. S. Lee, R. D. Schmidt and A. Mitchell, Synthesis and Scale-Up of 2,6-diamino-3,5-dinitropyrazine-1-oxide (LLM 105) and 2,6-diamino-3,5-dinitropyridine-1-oxide (ANPyO), Submitted to PEP (2005).
4 J. R. Kolb and H. F. Rizzo, Prop. Expl. Pyrotech., 4 (1979) 10.
5 L. R. Simpson and M. F. Foltz, LLNL Small-scale Drop-hammer Impact Sensitivity Test, LLNL Report UCRL-ID-119665 (Jan. 1005).
6 C. B. Skidmore, T. A. Butler and C. W. Sandoval, The Elusive Coefficients of Thermal Expansion in

PBX 9502, Los Alamos National Lab Communication, January 2003, LA-14003.
7 R. D. Gilardi and R. J. Butcher, Acta Cryst., E57 (2001) 657.
8 S. M. Marcus and R. L. Blaine, Thermochim. Acta, 243 (1994) 231.
9 Modulated DSC Compendium, Basic Theory and Experimental Conditions, TA Applications Brief, TA Instruments, New Castle, Delaware.
10 R. K. Weese, Thermochim. Acta, 429 (2005) 119.
11 Anonymous, TA Instruments, TA Applications Brief, TA 019, 1998, New Castle, DE.
12 Anonymous, TA Instruments, TMA 2940 Manual, 1996, TA Instruments, New Castle, DE.
13 L. R. Simpson and M. F. Foltz, LLNL Small-scale Friction Sensitivity (B.A.M.) Test, LLNL Report UCRL-ID-124563 (Jun. 1996).
14 L. R. Simpson and M. F. Foltz, LLNL Small-scale Static Spark Machine: Static Spark Sensitivity Test, LLNL Report UCRL-ID-135525 (Aug. 1999).
15 H. E. Kissinger, Anal. Chem., 29 (1957) 1702.
16 H. L. Friedman, J. Polym. Sci., C6 (1964) 183.
17 A. K. Burnham, J. Therm. Anal. Cal., 60 (2000) 895.
18 J. L. Maienschein and F. Garcia, Thermochim. Acta, 384 (2002) 71.
19 S. Gupa, S. P. Felix and P. Soni, Thermochim. Acta, 399 (2003) 153.

DOI: 10.1007/s10973-006-8163-4